THE JOURNAL OF PHYSICAL CHEMISTRY Letters

Letter

Cite This: J. Phys. Chem. Lett. 2019, 10, 144−149

pubs.acs.org/JPCL

Photoelectrons Are Not Always Quite Free

Jarrett L. Mason, Josey E. Topolski, Joshua Ewigleben, Srinivasan S. Iyengar,* and Caroline Chick Jarrold*

Department of Chemistry, Indiana University, 800 East Kirkwood Avenue, Bloomington, Indiana 47405, United States

ABSTRACT: The photoelectron spectra of Sm_2O^- obtained over a range of photon energies exhibit anomalous changes in relative excited-state band intensities. Specifically, the excited-state transition intensities increase relative to the transition to the neutral ground state with decreasing photon energy, the opposite of what is expected from threshold effects. This phenomenon was previously observed in studies on several Sm-rich homo- and heterolanthanide oxides collected with two different harmonic outputs of a Nd:YAG (2.330 and 3.495 eV) [*J. Chem. Phys.* **2017**, *146*, 194310]. We relate these anomalous intensities to populations of ground and excited anionic and neutrals states through the inspection of time-dependent perturbation theory within the adiabatic and sudden limits and for the first time show that transition intensities in photoelectron spectroscopy have a deep significance in gauging participation from excited states. We believe our results will have significance in the study of other electron-rich systems that have especially high density of accessible spin states.

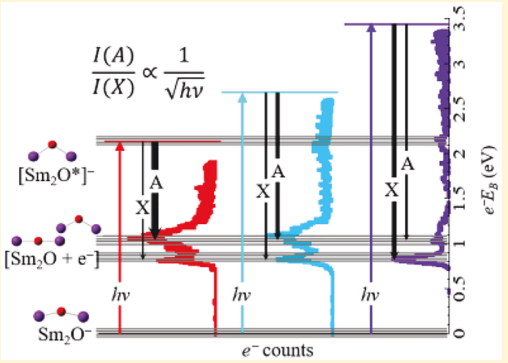

A recent report on the photoelectron (PE) spectra of several small $Sm_2O_y^-$ and mixed $SmCeO_y^-$ clusters noted that excited-state bands observed in the PE spectra of Sm_2O^- and $Sm_2O_2^-$ were more intense when the spectrum was measured with lower photon energy (2.330 eV, versus 3.495 eV).[1] This effect, which is the opposite of what is expected based on the Wigner threshold law,[2] was additionally observed in the PE spectra of larger $Sm_xCe_{3-x}O_y^-$ (x = 1−3; y = 2, 3) clusters[3] in which the average metal center oxidation state is ≤+2. The effect is increasingly pronounced as the average oxidation state is decreased. It was not observed for homometallic $Ce_xO_y^-$ homologues, suggesting that the exceptionally high density of spin states in Sm centers is somehow involved in this phenomenon. Ce and Sm, both lanthanoids, differ in the 4f subshell occupancy in these clusters, with Ce having a singly occupied 4f subshell, and Sm having between $4f^5$ and $4f^6$, depending on the specific $Sm_xCe_{n-x}O_y$/$Sm_xCe_{n-x}O_y^-$ composition (n = 2, 3, $1 \le x \le n$, $y \le n$).[3]

Excited anion states embedded in the detachment continuum can cause photon-energy-dependent intensity anomalies. A simple example of this effect was recently provided by Dao and Mabbs[4] in the vibrationally resolved PE imaging spectrum of AgF^-, which supports a dipole-bound state just below the AgF + e^- detachment continuum. Any vibrationally excited levels of the dipole-bound state that lie above the detachment continuum can autodetach via vibrational relaxation ($\Delta v = -1$ propensity rule), resulting in an enhancement of the electron signal associated with that particular $v' - 1$ neutral level. A variation on this theme has also been observed in our own laboratory in the PE spectrum of the O_2^-·benzene van der Waals complex.[5] The enhancement of the broad PE signal peaked at electron kinetic energy, $e^-E_K \approx 1$ eV, which coincides with the $O_2(^1\Delta_g)$·benzene + e^- ← $O_2^-(^2\Pi_g)$·benzene + $h\nu$ (3.49 eV) transition, which was attributed to resonance with a temporary anion state of benzene at e^-E_K = 1.12 eV.[6] In both of these cases, the photoelectron angular distrubution (PAD) of the signal enhanced by resonance with a quasibound anion state is more isotropic than direct detachment transitions.

In contrast, the enhanced excited-state transitions observed in the PE spectra of $Sm_xCe_{n-x}O_y^-$ clusters do not exhibit any significant change in PAD with photon energy, and the fact that they occur in a number of Sm-containing clusters with different compositions makes the prospect of a coincidental resonance at 2.330 eV seem remote. To further probe the origin of these effects, we have collected PE spectra of Sm_2O^-, the simplest molecule exhibiting this behavior, with eight photon energies ranging from 2.066 to 3.495 eV. On the basis of a previous study,[1] the ground electronic state of Sm_2O^- is a slightly bent, C_{2v} structure in a $^{14}B_2$ electronic state. Neutral Sm_2O is predicted to have a small, or no, dipole moment because it is a nearly linear or linear molecule (depending on the electronic state), and the Sm centers have a $4f^6$ subshell occupancy.[1]

We note here that in the case of molecules with exceptionally complex electronic structures, such as cases where the gaps are on the order of a few-tenths of an electronvolt among spin-polarized electronic states and where the true electronic structure may be expected to be multideterminantal, the density functional theory (DFT)

Received: October 25, 2018
Accepted: December 20, 2018
Published: December 20, 2018

DOI: 10.1021/acs.jpclett.8b03253
J. Phys. Chem. Lett. 2019, 10, 144−149

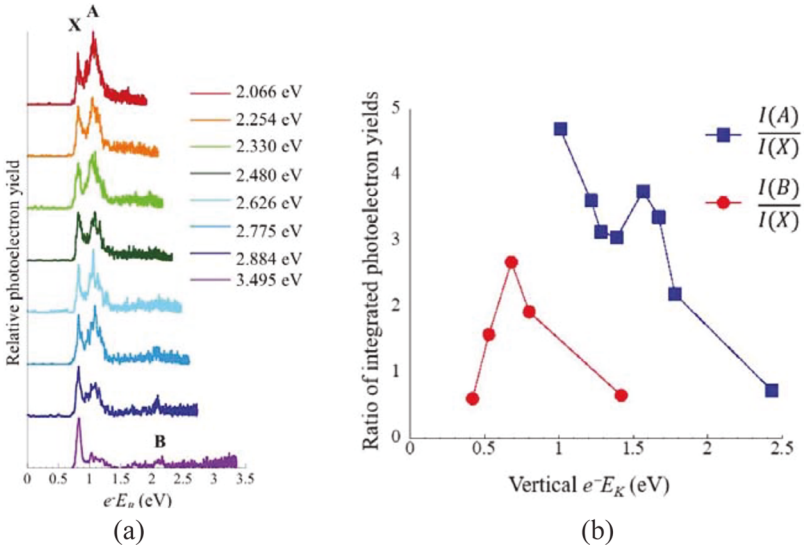

Figure 1. (a) PE spectra of Sm_2O^- obtained using the photon energies indicated. (b) Relative integrated intensities of excited-state transitions, A and B, to the ground-state transition, X, measured at different photon energies. The horizontal axis corresponds the electron kinetic energy (e^-E_K) associated with the maximum intensity of the excited-state bands, which decreases with decreasing photon energy. A similar trend is also seen as a function of incident photon energy.

results will need to be considered with caution, and we take these to be qualitative. In fact, for Sm_2O^-, there are numerous close-lying electronic states associated with the 12 unpaired (ferromagnetically or antiferromagnetically coupled) electrons occupying 14 molecular orbitals (MOs) arising from the 7 4f orbitals localized on each of the Sm centers and the 3 electrons (2 in the case of the neutral) occupying the nearly degenerate in-phase and out-of-phase combinations of the 6s orbitals, which can have parallel or opposite spins to the electrons in the 4f subshell. In addition, there are 10 nearly degenerate, unoccupied, low-lying MOs arising from the five 5d orbitals in the two Sm centers. Therefore, whereas DFT calculations may converge on several states associated with the $4f_a^6 4f_b^6 \sigma_{6s_a-6s_b}{}^2 \sigma_{6s_a-6s_b}{}^*$ superconfiguration of $Sm_aOSm_b^-$ within a narrow energy window, there are inevitably ca. 100 heavily mixed states within that window. Likewise, there are equally numerous mixed states lying in a narrow window of energy for the excited $4f_a^6 4f_b^6 \sigma_{6s_a-6s_b} \sigma_{6s_a-6s_b}{}^* x_{5d_a-5d_b}$ $(x = \sigma, \pi, \delta)$ anion superconfiguration and the low-lying $4f_a^6 4f_b^6 \sigma_{6s_a-6s_b} \sigma_{6s_a-6s_b}{}^*$ neutral superconfiguration.

With that caveat, in the $^{14}B_2$ electronic state of Sm_2O^- found computationally in previous DFT calculations, given the singly occupied HOMO ($\sigma_{6s_a-6s_b}{}^*$) and nearly degenerate, doubly occupied HOMO−1 ($\sigma_{6s_a-6s_b}{}^2$), transitions to the 15-tet and two 13-tet states accessed by the one-electron transition from these two orbitals should lie very close in energy. The very numerous and densely packed transitions associated with detachment from the 4f subshell should have comparatively small cross sections.[7] However, the apparent increase in transitions to excited states with decreased photon energy suggests that as the anionic system evolves in time under the influence of external field, the outgoing PE and remnant neutral-like species are coupled due to the proximity of excited states. The extent and scope of interaction between the outbound PE and remnant neutral-like species are governed by (a) the external photon energy that determines the outgoing electronic momentum and (b) the relatively high density of spin states available in these systems, both of which together influence the time scale of the interaction between the outbound electron and remnant neutral.

To explain the observed results, we consider in this Letter three limiting cases: (i) The first case is where the photon energy is high and then the photodetachment may be considered close to being a sudden process,[8] where the remnant-neutral-like state remains "frozen" in its initial configuration. (ii) In the second case, the photon energy is low and the photodetachment is adiabatic. Here the outbound electron has maximal opportunity to interact with the remnant neutral during the dissociation process, facilitated by the high density of spin states, and could involve weakly bound intermediates. (iii) Finally, intermediate photon energies lead to a more complicated description that may require explicit time evolution of the anionic system. We find that these limiting cases provide an appropriate description of the photodetachment process and are of significance to all similar processes in systems with a high density of spin states.

Experimental PE Intensities That Bear the Signature of the Complex Photoelectron Relaxation Process. The spectra were measured using an apparatus previously described in detail.[9−11] The spectra of Sm_2O^- are presented in terms of electronic binding energies (e^-E_B) using the electron kinetic energies (e^-E_K)

$$e^-E_K = h\nu - EA - T_e^{neutral} + T_e^{anion} = h\nu - e^-E_B \qquad (1)$$

yielding spectra with transition energies that are independent of photon energy and facilitating a more direct visual comparison of the band intensities. The e^-E_B values reflect the energy difference between the final neutral state, the electron affinity, and the initial anion state, as reflected in eq 1.

Figure 1a shows the new PE spectra of Sm_2O^- obtained using photon energies ranging from 3.495 to 2.066 eV, all measured with ∼5 mJ/pulse (previously reported 2.330 and 3.495 eV spectra were measured using approximately 20−30 mJ/pulse). As before,[1] the spectrum obtained at 3.495 eV exhibits at least three distinct electronic transitions labeled X, A, and B, with vertical detachment energies (the energy at

DOI: 10.1021/acs.jpclett.8b03253
J. Phys. Chem. Lett. 2019, 10, 144−149

Table 1. Lower-Lying Electronic Energy States for the Anionic and Neutral Systems Obtained from DFT[1a]

Sm_2O^- Electronic State	$c_i(0)$ values from Boltzmann weights
$^{12}B_2$	0.015
$^{2}A'$	0.119
$^{14}B_2$	0.867

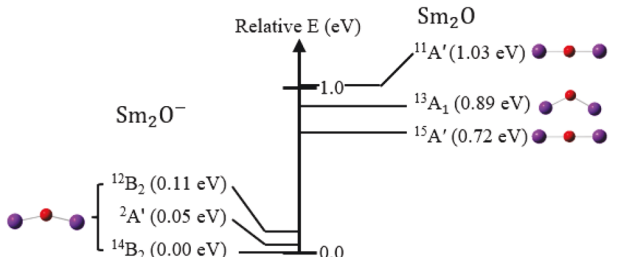

[a]Note that the symmetry of several of the anion and neutral states was not identified as C_{2v} in the calculations. The corresponding Boltzmann weights at 300 K contribute to the coefficients in eq 2.

which the band reaches maximum intensity) of 0.80(1), 1.06(3), and 2.08(1) eV. Band X is significantly higher in intensity than bands A and B in the spectrum obtained with 3.495 eV; however, the plot clearly shows that the relative intensity of band A increases as the photon energy is decreased. No distinct, consistent vibrational structure in any of the transitions emerges with decreased photon energy, despite the experimental resolution increasing with decreasing e^-E_K.[11] No assignment of band B was made, beyond tentatively attributing it to a shakeup transition. We note here that numerous PE spectra of lanthanide suboxides have exhibited a similar low-intensity transition, with similar e^-E_B values.[12−15]

A plot of the ratio of the excited-state integrated PE yields relative to band X as a function of vertical e^-E_K (the energy at which the band intensity is maximum) is shown in Figure 1b. The most striking aspect depicted in Figure 1b is that the probability of populating the excited neutral states associated with band A increases significantly relative to the probability of populating the ground neutral state associated with band X at low photon energies. As the photon energy is increased, there is an almost monotonic decrease in this ratio, with an attending oscillation at e^-E_K (A) between 1.4 and 2 eV. The integrals were performed on the raw electron yield versus drift time data plots over time windows that correlate to the same set of e^-E_B intervals. Note that band B is affected by the instrumental cutoff, 0.5 eV, as the photon energy decreases from 3.49 eV.

Adiabatic and Sudden Descriptions of the Anomalous PE Spectra. In the higher energy limit, the electron is ejected from the anion with a relatively large outbound momentum, and the electron and resulting neutral molecule do not interact, behaving independently. Hence the neutral appears relatively frozen in its initial configuration. On the contrary, low- and intermediate-energy photons result in an electron detachment process that is protracted in time, allowing the outbound PE to closely interact with the "time-evolving" states of the remnant (neutral-like) species, thereby strongly influencing both final states. Furthermore, such a time evolution is facilitated by the time-dependent polarizing field, and thus the final detached PE state has resulted after its electronic state has evolved while interacting with the remnant neutral-like molecule.

To maintain generality, we consider the initial state of the anionic system as a wavepacket composed of multiple anionic spin states, $\{S_i\}$, inside and an energy window, E_w

$$|\Phi^-(0)\rangle \equiv \sum_{i\in E_w} c_i(0)|\Psi^-_{i,S_i}\rangle \tag{2}$$

where the parenthetic "(0)" is initial time and $\{|\Psi_{i,S_i}{}^-\rangle\}$ refers to anionic spin states. The coefficients of the states in eq 2 may be thermally derived at initial time or may depend on other experimental considerations. By "thermal", we imply that the initial conditions of the experiment may populate some excited anionic electronic states in addition to the ground electronic state given that the gap between the electronic states is small, as seen from Table 1. In Table 1, we also show the $c_i(0)$ values derived from Boltzmann factors at 300 K, and hence the $^2A'$ anionic state has a 12% Boltzmann population at 300 K. Higher energy excited states of the anion are considered later in the discussion as a part of our analysis.

Once the initial state is created as per eq 2, this initial state, $|\Phi^-(0)\rangle$, defines a closed system that evolves in time under the influence of the anionic Hamiltonian and the external field, which imparts an outbound momentum, or "kick", to the departing PE. Under the conditions that the external field is weak, we may use first-order time-dependent perturbation theory[8] to study the evolution of the anionic state as the PE departs. Thus the probability of finding the time-evolving anionic state in a specific projectile momentum state with kinetic energy, $j_k = \hbar^2k(t)^2/2m$, and angular momentum, $|J\rangle$ and aligned along the neutral state, $\Psi_{\alpha,S_\alpha}{}^0$, is

$$|\langle J; j_k; \Psi^0_{\alpha,S_\alpha}|\Phi^-(\tau)\rangle|^2 = \frac{1}{\hbar^2}\left|\sum_{i\in E_w} c_i(0)\int_{t'=0}^{t'=\tau} dt'\, e^{i2\pi\nu t'}\langle J; j_k; \Psi^0_{\alpha,S_\alpha}|V(t')|\Psi^-_{i,S_i}\rangle\right|^2 \tag{3}$$

Here $V(t')$ is the time-dependent perturbation on the system due to incident photon energy with frequency, ν, with "τ" being the duration of interaction time between the outbound electron and remnant neutral. The right-hand side of eq 3 depends on the incident photon energy (through the presence of ν) and the outbound PE kinetic energy (through the presence of outbound momentum state, j_k). If we assume that the incident photon imparts an outbound momentum to the PE and the time dependence of the field is negligible during the time of dissociation, then $V(t) = T_\beta + V^\beta_{eN} + V^\beta_{ee}$, where the outgoing electron is labeled as "β" and the time dependence of $V(t)$ arises from the time dependence of the position of β, which affects the term $[V^\beta_{eN} + V^\beta_{ee}]$. Furthermore, because the e^-E_K is proportional to the incident photon energy, the time of interaction, τ, is inversely proportional to the square root of the photon energy, and eq 3 may then be rewritten as

DOI: 10.1021/acs.jpclett.8b03253
J. Phys. Chem. Lett. 2019, 10, 144−149

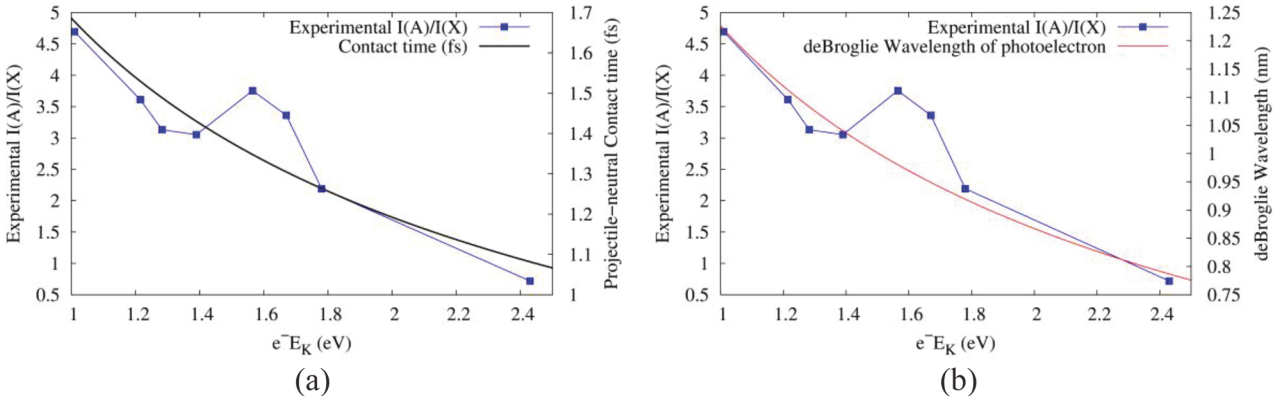

Figure 2. Projectile-remnant neutral contact time, $\propto \sqrt{m_e}/\sqrt{2h\nu}$, and the corresponding photoelectron de Broglie wavelength are shown with experimental intensity ratios as a function of photoelectron kinetic energy. The pronounced oscillation in experimental intensity behavior appears to be due to a resonance between the outgoing electron and remnant neutral.

$$\left|\left\langle J; j_k; \Psi^0_{\alpha,S_\alpha}\middle|\Phi^-\left(\frac{a}{\sqrt{h\nu}}\right)\right\rangle\right|^2 = \frac{1}{\hbar^2}\left|\sum_{i\in E_w} c_i(0)\int_0^{a/\sqrt{h\nu}} dt' e^{i2\pi\nu t'}\langle J; j_k; \Psi^0_{\alpha,S_\alpha}\middle|T_\beta + V^\beta_{eN} + V^\beta_{ee}\middle|\Psi^-_{i,S_i}\rangle\right|^2 \quad (4)$$

where a is a constant that captures the approximate spatial range over which the outbound PE feels the effect of the remnant neutral. Because the contribution from excited state to eq 2 is only on the order of 12%, we may approximate the right side of eq 4, using the ground anionic state as

$$\left|\left\langle J; j_k; \Psi^0_{\alpha,S_\alpha}\middle|\Phi^-\left(\frac{a}{\sqrt{h\nu}}\right)\right\rangle\right|^2 \approx \frac{1}{\hbar^2}\left|\int_0^{a/\sqrt{h\nu}} dt' e^{i2\pi\nu t'}\langle J; j_k; \Psi^0_{\alpha,S_\alpha}\middle|T_\beta + V^\beta_{eN} + V^\beta_{ee}\middle|\Psi^-_{0,S_0}\rangle\right|^2 \quad (5)$$

which in the adiabatic limit reduces to

$$\left|\left\langle J; j_k; \Psi^0_{\alpha,S_\alpha}\middle|\Phi^-\left(\frac{a}{\sqrt{h\nu}}\right)\right\rangle\right|^2 = \frac{1}{\pi^2\nu^2\hbar^2}\left|\frac{d}{dt}\langle J; j_k; \Psi^0_{\alpha,S_\alpha}\middle|T_\beta + V^\beta_{eN} + V^\beta_{ee}\middle|\Psi^-_{i,S_i}\rangle\right|^2 \sin^2\left(\pi a\sqrt{\frac{\nu}{h}}\right) \quad (6)$$

and in the sudden limit

$$\left|\left\langle J; j_k; \Psi^0_{\alpha,S_\alpha}\middle|\Phi^-\left(\frac{a}{\sqrt{h\nu}}\right)\right\rangle\right|^2 = \frac{1}{4\pi^2\nu^2\hbar^2}\left|\langle J; j_k; \Psi^0_{\alpha,S_\alpha}\middle|T_\beta + V^\beta_{eN} + V^\beta_{ee}\middle|\Psi^-_{i,S_i}\rangle\right|^2 \quad (7)$$

For intermediate photon energies, it is the time scale of the outgoing electron, which is $\propto \frac{1}{\sqrt{e^-E_K}} \approx \frac{a}{\sqrt{h\nu}}$, that dictates how the anionic states couple, and, more precisely, how the outward momentum state couples to the remnant "neutral-like-state". This can be seen from eq 5 in the weak field limit

$$\left|\left\langle J; j_k; \Psi^0_{\alpha,S_\alpha}\middle|\Phi^-\left(\frac{a}{\sqrt{h\nu}}\right)\right\rangle\right|^2 \approx \frac{1}{\hbar^2}\left|\int_0^{a/\sqrt{h\nu}} dt' \langle J; j_k; \Psi^0_{\alpha,S_\alpha}\middle|T_\beta + V^\beta_{eN} + V^\beta_{ee}\middle|\Psi^-_{0,S_0}\rangle\right|^2 \quad (8)$$

The integral of the matrix element is inversely proportional to the time scale of departure of the outbound PE.[8] Larger time scales (lower e^-E_K) facilitated by a correspondingly high density of anionic states result in greater coupling between anionic states inside E_w and the states belonging to the remnant neutral and the PE. As a result, we introduce the contact time as the duration of time over which the two entities interact, and this quantity is inversely proportional to the square root of the photon energy (as seen from eqs 4 and 5); we then compare this contact time, in Figure 2a, with the intensity ratios obtained from experiment. As noted, the ratio of intensities tracks the contact time fairly well apart from the oscillation at ∼1.6 eV. We also consider the de Broglie wavelength of the outgoing PE in Figure 3b, and this again tracks the ratio of intensities much like the contact time.

What are the reasons for the oscillations in the intensity ratio seen in the experiment? These oscillations seen in the experiment are likely caused by the presence of resonances between the anionic electronic state and the composite outbound electron-remnant neutral state. For example, bands "X" and "A" are roughly at 0.8 and 1.0 eV in Figure 1a. At these e^-E_B values, there are several combinations of anion to neutral electronic states possible, as seen in Table 1. As per eqs 2 and 4, one would expect all possible transitions to contribute to the experimental PE spectrum. These include contributions from $^{14}B_2 \rightarrow {}^{15}A'$ and $^{12}B_2 \rightarrow {}^{13}A_1$ for the 0.8 eV binding energy and $^{14}B_2 \rightarrow {}^{13}A_1$ and transitions originating from the $^2A'$ state of the anion to antiferromagnetic spin states of the neutral that are generally hard to converge in most standard electronic structure calculations and would contribute to the 1 eV binding energy. Furthermore, as illustrated in Figure 3, these transitions along with the outbound PE energy together are potentially resonant with multiple quasibound anionic states calculated to be between 2 and 2.5 eV above the ground state of the anion with the $4f^6_a 4f^6_b \sigma_{6s_a-6s_b} \sigma_{6s_a-6s_b}{}^* x_{5d_a-5d_b}$ superconfiguration ($x = \sigma, \pi, \delta$ MOs from the two sets of Sm 5d orbitals), a very small sampling of which converged, and are

DOI: 10.1021/acs.jpclett.8b03253
J. Phys. Chem. Lett. 2019, 10, 144−149

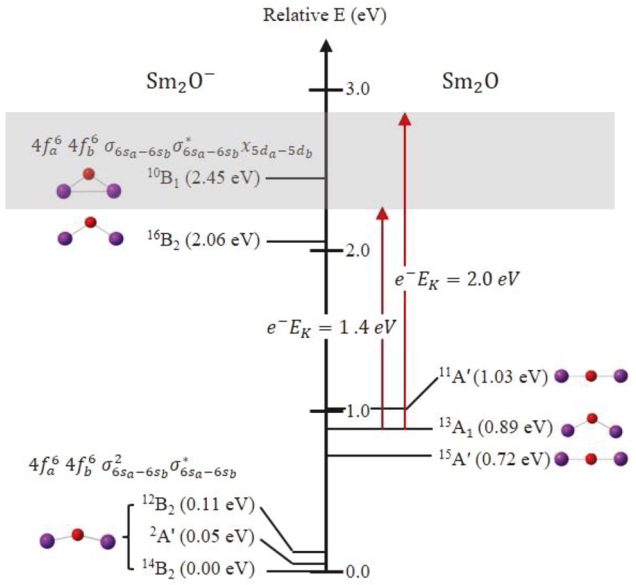

Figure 3. Excited states of the anion in the energy range near or coinciding with the oscillations in the relative intensities of bands X and A as a function of band A vertical e^-E_K for $1.4 < e^-E_K < 2$ eV. The excited states of the anion lying above 2 eV are expected to be numerous and close-lying due to the near-degeneracy of MOs with Sm 5d character.

shown in Figure 3. The coherent oscillations between this available set of states is expected to be captured through the oscillations in the experimentally measured intensity ratios. Similar coherent oscillations have been noted in several fundamental gas-phase reactions, such as isotopic and heavier variations of $H + H_2 \rightarrow H_2 + H$ (ref 16) and $F + H_2 \rightarrow HF + H$ (refs 17 and 18), where, when the energy of the system is increased, the reaction rates do not follow a monotonic trend. The reason for the oscillations in molecular reaction probabilities is again due to the existence of bound state in resonance with the unbound dissociative state in those cases. Similar behavior has also been seen in biological enzymes where orthogonal vibrational modes act as a switch to tailor reaction dynamics.[19]

To summarize, we have extended previous anion PE spectroscopic studies on small Sm-containing clusters in low oxidation states, which have exceptionally complex electronic structures, to include a wider range of photon detachment energies. The new results show continued increases in the relative excited-state transition intensities, including a broad oscillation, with decreasing photon energy, an effect that is opposite to threshold law behavior. We present a theoretical platform for introducing the time evolution of the electron-neutral complex in protracted detachment events that maps onto the general experimentally observed trends in relative excited-state intensities.

AUTHOR INFORMATION

Corresponding Authors

*E-mail: cjarrold@indiana.edu. Tel: 812-856-1190 (C.C.J.).
*E-mail: iyengar@indiana.edu. Tel: 812-856-1875 (S.S.I.).

ORCID

Srinivasan S. Iyengar: 0000-0001-6526-2907
Caroline Chick Jarrold: 0000-0001-9725-4581

Notes

The authors declare no competing financial interest.

ACKNOWLEDGMENTS

This work was supported by the U.S. Department of Energy, Office of Science, Basic Energy Sciences, CPIMS Program under award no. DE-FG02-07ER15889 at Indiana University (to C.C.J.) and through the National Science Foundation Grant CHE-1665336 (to S.S.I.).

REFERENCES

(1) Kafader, J. O.; Topolski, J. E.; Marrero-Colon, V.; Iyengar, S. S.; Jarrold, C. C. The Electron Shuffle: Cerium Influences Samarium 4f Orbital Occupancy in Heteronuclear Ce-Sm Oxide Clusters. *J. Chem. Phys.* **2017**, *146*, 194310.

(2) Wigner, E. P. On the Behavior of Cross Sections Near Thresholds. *Phys. Rev.* **1948**, *73*, 1002−1009.

(3) Topolski, J. E.; Kafader, J. O.; Marrero-Colon, V.; Iyengar, S. S.; Hratchian, H. P.; Jarrold, C. C. Exotic Electronic Structures of $Sm_xCe_{3-x}O_y$ (x = 0−3; y = 2−4) Clusters, and the Effect of High Neutral Density of Low-lying States on Photodetachment Transition Intensities. *J. Chem. Phys.* **2018**, *149*, 054305.

(4) Dao, D. B.; Mabbs, R. The Effect of the Dipole Bound State on AgF^- Vibratinoally Resolved Photodetachment Cross Sections and Photoelectron Angular Distributions. *J. Chem. Phys.* **2014**, *141*, 154304.

(5) Patros, K. M.; Mann, J. E.; Jarrold, C. C. Photoelectron Imaging Spectra of O_2^-·VOC and O_4^-·VOC Complexes. *J. Phys. Chem. A* **2016**, *120*, 7828−7838.

(6) Jordan, K. D.; Burrow, P. D. Temporary Anion States of Polyatomic Hydrocarbons. *Chem. Rev.* **1987**, *87*, 557.

(7) O'Malley, S. M.; Beck, D. R. Calculation of Ce^- Binding Energies by Analysis of Photodetachment Partial Cross Sections. *Phys. Rev. A: At., Mol., Opt. Phys.* **2006**, *74*, 042509.

(8) (a) Messiah, A. *Quantum Mechanics*; John Wiley & Sons, Inc.: New York, 1966. (b) Davydov, A. S. *Quantum Mechanics*; Addison-Wesley Publishing Company, Inc.: Reading, MA, 1965.

(9) Moravec, V. D.; Jarrold, C. C. Study of the Low-Lying States of NiO^- and NiO Using Anion Photoelectron Spectroscopy. *J. Chem. Phys.* **1998**, *108*, 1804−1810.

(10) Waller, S. E.; Mann, J. E.; Jarrold, C. C. Asymmetric Partitioning of Metals among Cluster Anions and Cations Generated via Laser Ablation of Mixed Aluminum/Group 6 Transition Metal Targets. *J. Phys. Chem. A* **2013**, *117*, 1765−1772.

(11) Felton, J. A.; Ray, M.; Jarrold, C. C. Measurement of the Electron Affinity of Atomic Ce. *Phys. Rev. A: At., Mol., Opt. Phys.* **2014**, *89*, 033407 1−5.

(12) Ray, M.; Felton, J. A.; Kafader, J. O.; Topolski, J. E.; Jarrold, C. C. Photoelectron Spectra of CeO^- and $Ce(OH)_2^-$. *J. Chem. Phys.* **2015**, *142*, 064305.

(13) Kafader, J. O.; Ray, M.; Jarrold, C. C. Photoelectron Spectrum of PrO^-. *J. Chem. Phys.* **2015**, *143*, 064305.

(14) Kafader, J. O.; Topolski, J. E.; Jarrold, C. C. Molecular and Electronic Structures of Cerium and Cerium Suboxide Clusters. *J. Chem. Phys.* **2016**, *145*, 154306.

(15) Weichman, M. L.; Vlaisavljevich, B.; DeVine, J. A.; Shuman, N. S.; Ard, S. G.; Shiozaki, T.; Neumark, D. M.; Viggiano, A. A. Electronic Structure of SmO and SmO^- via Slow Photoelectron Velocity-Map Imaging Spectroscopy and Spin-Orbit CASPT2 Calculations. *J. Chem. Phys.* **2017**, *147*, 234311.

(16) Dai, D.; Wang, C. C.; Harich, S. A.; Wang, X.; Yang, X.; Chao, S. D.; Skodje, R. T. Interference of Quantized Transition-state Pathways in the $H + D_2 \rightarrow D + HD$ Chemical Reaction. *Science* **2003**, *300*, 1730−1734.

(17) Neumark, D. M.; Wodtke, A. M.; Robinson, G. N.; Hayden, C. C.; Lee, Y. T. Experimental Investigation of Resonances in Reactive Scattering- the $F + H_2$ Reaction. *Phys. Rev. Lett.* **1984**, *53*, 226−229.

DOI: 10.1021/acs.jpclett.8b03253
J. Phys. Chem. Lett. 2019, 10, 144−149

(18) Skodje, R. T.; Skouteris, D.; Manolopoulos, D. E.; Lee, S.-H.; Dong, F.; Liu, K. Resonance-mediated Chemical Reaction: F + HD → HF + D. *Phys. Rev. Lett.* **2000**, *85*, 1206−1209.
(19) Phatak, P.; Venderley, J.; deBrota, J.; Li, J.; Iyengar, S. S. Active Site Dynamical Effects in the Hydrogen Transfer Rate-limiting Step in the Catalysis of Linoleic Acid by Soybean Lipoxygenase-1 (SLO-1): Primary and Secondary Isotope Contributions. *J. Phys. Chem. B* **2015**, *119*, 9532−9546.

DOI: 10.1021/acs.jpclett.8b03253
J. Phys. Chem. Lett. 2019, 10, 144−149